New Physics: Sae Mulli,
Vol. 67, No. 11, November 2017, pp. 1272∼1278
http://dx.doi.org/10.3938/NPSM.67.1272

Electrical and Ferroelectric Properties of Rare-earth-doped $Na_{0.5}Bi_{4.0}RE_{0.5}Ti_4O_{15}$ (RE = Eu, Gd and Dy) Thin Films

Min Hwan KWAK
Department of Electrical Engineering, Changwon Moonsung University, Changwon 51410, Korea

Chinnambedu Murugesan RAGHAVAN · Sang Su KIM · Won-Jeong KIM*
Department of Physics, Changwon National University, Changwon 51140, Korea

(Received 22 September 2017 : revised 16 October 2017 : accepted 16 October 2017)

A study of the structural, electrical and ferroelectric properties of layered Aurivillius-type $Na_{0.5}Bi_{4.5}Ti_4O_{15}$ (NaBTi) and $Na_{0.5}Bi_{4.0}RE_{0.5}Ti_4O_{15}$ (RE = Eu, Gd and Dy) thin films is reported. These films were fabricated on Pt-coated Si(100) substrates by using a chemical solution deposition method followed by a heat treatment. The rare-earth elements used as dopants, such as Eu, Gd and Dy, were found to be effective in improving the leakage current densities and the ferroelectric properties of the layered $Na_{0.5}Bi_{4.5}Ti_4O_{15}$ thin films without affecting their original Aurivillius structures. Based on the measured ferroelectric polarization-electric field ($P-E$) hysteresis loops, we found that the Gd-doped NaBTi thin film, among all the films, exhibited the highest ferroelectric remnant polarization of $2P_r$ = 37.4 μC/cm^2 and a low coercive electric field of $2E_c$ = 187 kV/cm at an applied electric field of 475 kV/cm. Furthermore, the lowest value of the leakage current density of 6.12×10^7 A/cm^2 at an applied electric field of 100 kV/cm was measured for the Gd-doped NaBTi thin film.

PACS numbers: 77.55.-g, 77.55.fp, 73.61.-r
Keywords: $Na_{0.5}Bi_{4.5}Ti_4O_{15}$ thin film, Chemical solution deposition, Microstructure, Electrical properties, Ferroelectric properties

I. INTRODUCTION

The extensive diversities in ferroelectric, piezoelectric and magneto-electric properties of bismuth layered structure ferroelectric (BLSF) compounds led to a wide variety of applications of these compounds in modern electronics industry. Generally, the fabrication of micro electro-mechanical system, sensor, actuator and non-volatile memory devices depends largely on this type of lead free ferroelectric materials [1–4]. In this regard, the Aurivillius phase $M_{0.5}Bi_{4.5}Ti_4O_{15}$ (M = Na and K) compounds that belong to the family of BLSFs have recently gained a great deal of technological interest owing to their superior ferroelectric and piezoelectric behaviors [5–8]. These compounds own many advantageous characteristics, namely, high fatigue endurance, large piezoelectric coefficient, toxic Pb-ion free chemical constituents and high transition temperature [9]. The BLSF compound, $Na_{0.5}Bi_{4.5}Ti_4O_{15}$ (NaBTi), has been considered a very promising material not only due to its high transition temperature, but also because of its large electromechanical quality factor [9,10]. The NaBTi has an orthorhombic structure comprising four layers of pseudo perovskite like units, $(Bi_{n-1}Ti_nO_{3n+1})^{2-}$ (n = 4), alternating with fluorite like units, bismuth oxide $(Bi_2O_2)^{2+}$ layers, and these building blocks are arranged along the c-axis [11,12]. The lighter Na-atoms replace a few Bi-atoms in the pseudo-perovskite unit of the orthorhombic structure. The NaBTi had been reported to undergo a phase transition from the ferroelectric phase ($A2_1am$) to the para-electric phase ($I4/mmm$) at 655 °C [12].

*E-mail: kwj@changwon.ac.kr

Despite many advantageous, the NaBTi is associated with certain limitations, such as large leakage current, low ferroelectric remnant polarization and large coercive field, which are necessary to overcome before using in practical devices. In order to mitigate these problems in BLSFs, the strategy of cationic doping using various rare-earth (RE) metal and transition metal elements has been widely investigated [2,7,13–16]. Particularly, doping with RE metal ions into the Bi-site of the BLSFs had been reported to be highly effective in enhancing ferroelectric remnant polarization and reducing leakage current density. For instance, doping with La^{3+}-ion into the Bi-site of the $Bi_4Ti_3O_{12}$ significantly increased the remnant polarization and fatigue endurance [17].

Doping with RE elements other than La into the Bi-site of the BLSFs is of interest due to certain structural distortions caused in the perovskite block [18]. It is believed that proper engineering of the Aurivillius BLSF structure through doping with appropriate RE metal ions can be helpful to improve the ferroelectric properties of NaBTi thin films. To this end, the RE metal ions, Eu, Gd and Dy have been used in the current study for doping of NaBTi thin films to improve both electrical and ferroelectric properties of the thin films. Since the ionic radii of the Eu^{3+}, Gd^{3+} and Dy^{3+} are smaller than that of the Bi^{3+}, these ions should be easily replace Bi ions in the NaBTi. Moreover, doping with the above-mentioned RE metal ions is highly promising in enhancing the ferroelectric polarization.

II. EXPERIMENTS

Chemical solution deposition method was used to deposit pure $Na_{0.5}Bi_{4.5}Ti_4O_{15}$ and $Na_{0.5}Bi_{4.0}RE_{0.5}Ti_4O_{15}$ (RE = Eu, Gd and Dy, represented as NaBEuTi, NaBGdTi and NaBDyTi, respectively) thin films on $Pt(111)/Ti/SiO_2/Si(100)$ substrates. The starting materials, viz. sodium nitrate [$NaNO_3$], bismuth nitrate pentahydrate [$Bi(NO_3)_3{\cdot}5H_2O$] and titanium isopropoxide [$Ti[OCH(CH_3)_2]_4$] were used for the basic precursor solutions. Europium nitrate pentahydrate [$Eu(NO_3)_3{\cdot}5H_2O$], gadolinium nitrate pentahydrate [$Gd(NO_3)_3{\cdot}5H_2O$] and dysprosium nitrate hydrate [$Dy(NO_3)_3{\cdot}xH_2O$] were used as a dopant to replace a part of Bi. 2-methoxy ethanol (2-MOE) [$CH_3OCH_2CH_2OH$] was used as solvent, and acetic acid [CH_3COOH] was used as catalyst. The $Na_{0.5}Bi_{4.5-x}RE_xTi_4O_{15}$ precursor solutions were prepared following the standard procedure, reported elsewhere [19]. Accordingly, sodium nitrate has been dissolved in 2-MOE on a hot-plate of 40 °C for a 30 min stirring. After adding acetic acid as catalyst, the solution has been stirred for another 30 min. Both bismuth nitrate pentahydrate and one of RE metal nitrates were added into the solution while stirring continuously for 2 h to improve homogeneity of the solutions. Ti precursor solution using titanium isopropoxide was prepared separately by mixing with 2-MOE and acetyl acetone [$CH_3COCH_2COCH_3$] in a glove box and stirred for an additional 1.5 h. Finally, both Ti-solution and the Na-Bi-RE solution have been mixed into the $Na_{0.5}Bi_{4.0}RE_{0.5}Ti_4O_{15}$ precursor solutions while stirring continuously for 3 h. For comparison with RE doped thin films, NaBTi thin film without dopant was fabricated from the NaBTi precursor solution prepared by the same procedure mentioned above. Due to the well-known volatility of Na and Bi at high temperature, 15% excessive Na and Bi solutions were used for thin film fabrication.

The NaBTi, NaBEuTi, NaBGdTi and NaBDyTi precursor solutions were coated on $Pt(111)/Ti/SiO_2/Si(100)$ substrates through spin coating (3000 rpm) for 20 s. The wet layer and substrate was prebaked at 200 °C and 360 °C for 5 min each to dry and/or eliminate organic impurities. This coating and baking process was repeated 15 times to obtain films with a desired film thickness. Finally, the entire coated layers were annealed at 500 °C and 700 °C for 3 min each by a rapid thermal annealing (RTA) method in oxygen environment to crystallize the layer. After fabrication of the films, adhesion between films and substrates were tested by a simple adhesive tape peeling method.

The structures of the NaBTi and the $Na_{0.5}Bi_{4.0}RE_{0.5}Ti_4O_{15}$ thin films were investigated by using an X-ray diffractometer (MiniFlex II, Rigaku, Japan) with CuK_α radiation. The surface and cross section morphologies were examined by scanning electron microscope (SEM) (MIRA II LMH, Tescan, Czech

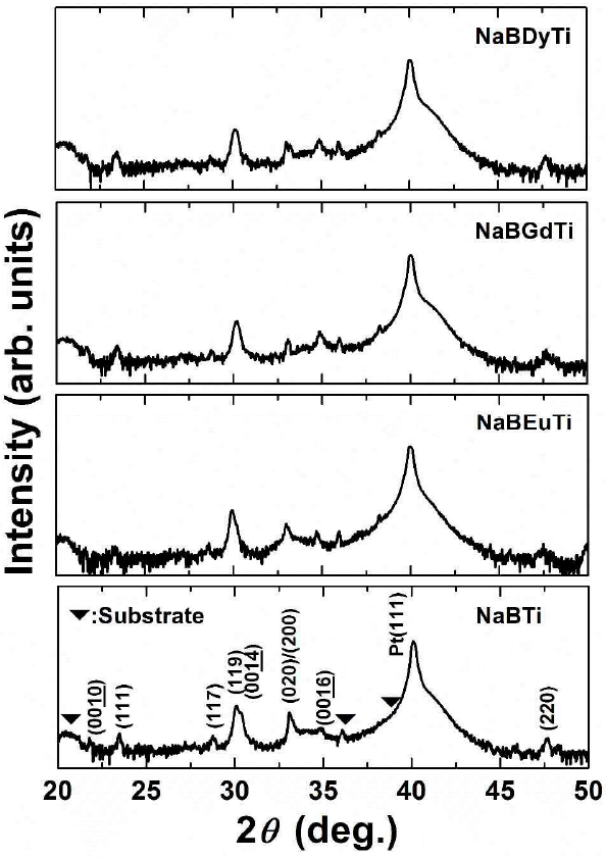

Fig. 1. XRD patterns of NaBTi, NaBEuTi, NaBGdTi and NaBDyTi thin films deposited on Pt(111)/Ti/SiO_2/Si(100) substrates.

Republic). Circular shape top Pt electrodes (1.54×10^{-4} cm^2) were prepared on the thin films by an ion sputter using a metal shadow mask to measure the electrical and ferroelectric properties of the films. Leakage current densities and ferroelectric properties of the thin films were studied by an electrometer (6517A, Keithley, USA) and a low-frequency impedance analyzer (4192A, HP, USA), respectively. A standard ferroelectric test system (Precision LC, Radiant Technologies Inc., USA) was used to investigate the ferroelectric hysteresis loops of the thin films.

III. RESULT AND DISCUSSION

The X-ray diffraction (XRD) patterns of the NaBTi, NaBEuTi, NaBGdTi and NaBDyTi thin films deposited on Pt(111)/Ti/SiO_2/Si(100) substrates are shown in Fig. 1. The indexed XRD patterns for the thin films

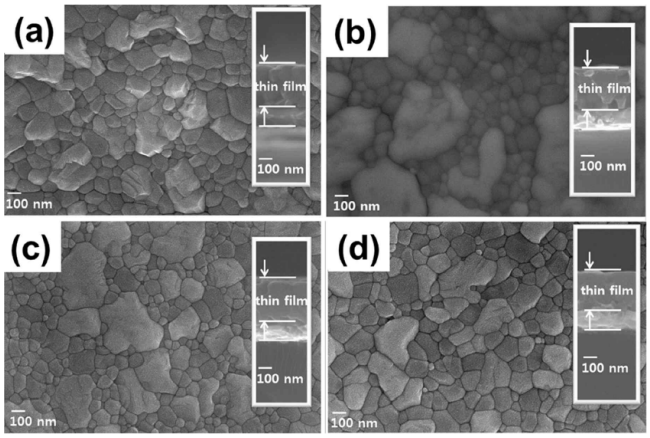

Fig. 2. Surface morphologies and cross-sectional micrographs of (a) NaBTi, (b) NaBEuTi, (c) NaBGdTi, and (d) NaBDyTi thin films.

agreed well with poly-crystalline Aurivillius phase orthorhombic symmetry with space group $A2_1am$ without any peaks related with secondary or impurity phases. This result indicated that the concentration of *RE* ions used for doping was not sufficient to make any significant change in the original crystal structure of the NaBTi thin film. However, the incorporation of the Eu^{3+}, Gd^{3+} and Dy^{3+}-ions into the Bi-site of the NaBTi led to a small strain in the crystal lattices, which were clearly revealed by the structural distortion in the $Na_{0.5}Bi_{4.0}RE_{0.5}Ti_4O_{15}$ thin films. The major diffraction peaks, such as (119) and (0014), of NaBTi exhibited peak separation, while those of $Na_{0.5}Bi_{4.0}RE_{0.5}Ti_4O_{15}$ were not separated but overlapped as a broad single peak. This strongly suggests that there are structural distortion in the *RE*-doped NaBTi thin films induced by doping the *RE* ions.

The surface morphologies and the cross-sectional micrographs of the NaBTi, NaBEuTi, NaBGdTi and NaBDyTi thin films are shown in Fig. 2. A study of surface morphologies clearly revealed a dense microstructure for all the thin films. From Fig. 2, the surface morphologies of the thin films resembled irregular shaped stones embedded on the wall. Furthermore, the thin films did not show any micro or macro pores and cracks on their surface morphologies. The NaBGdTi and the NaBDyTi thin films showed uniformly distributed grains compared with the NaBEuTi thin film. The thickness of the thin films, as estimated from the cross-sectional micrographs, was ∼300 nm.

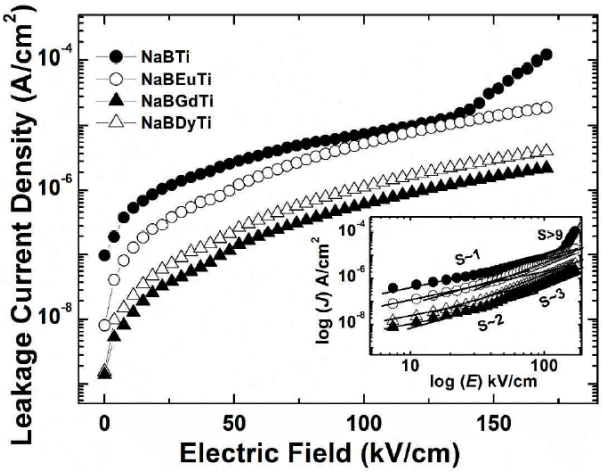

Fig. 3. Leakage current densities of NaBTi, NaBEuTi, NaBGdTi and NaBDyTi thin films. The inset shows log(J)-log(E) characteristics of the thin films.

The effect of doping of the Eu^{3+}, Gd^{3+} and Dy^{3+}-ions on the leakage currents of the $Na_{0.5}Bi_{4.0}RE_{0.5}Ti_4O_{15}$ thin films was further investigated. Fig. 3 exhibits the leakage current densities of the thin films measured at various *dc* applied electric field. The leakage current densities measured at 100 kV/cm for the NaBTi, NaBEuTi, NaBGdTi and NaBDyTi thin films were 7.38×10^{-6}, 5.30×10^{-6}, 6.12×10^{-7} and 1.12×10^{-6} A/cm^2, respectively. In ferroelectric thin films, presence of ionic vacancies and poor microstructure are generally considered as the major reasons for large leakage current. The thermal treatments, such as drying and annealing of the NaBTi thin film led to the evaporation of the Na and the Bi-atoms having high vapor pressures, which in turn resulted in cationic vacancies accompanied with oxygen vacancies [19,20]. Thus, the ionic vacancies in the NaBTi thin film can act as free charge carriers to generate large leakage current density. Doping of the *RE*-ion can compensate the vacancies generated by the trivalent Bi-ion and stabilize the pseudo-perovskite block in the Aurivillius structure [13,16]. The low leakage current densities for the $Na_{0.5}Bi_{4.0}RE_{0.5}Ti_4O_{15}$ thin films can be attributed to the presence of low concentration of oxygen vacancies in comparison to the NaBTi thin film. Among all the thin films, the Gd-doped film, *i.e.*, the NaBGdTi thin film exhibited the lowest leakage current density of 6.12×10^{-7} A/cm^2, which is about one order of magnitude lower than that of the NaBTi thin film. When compared with Gd^{3+} and Dy^{3+}-ions, the doping with Eu^{3+}-ion did not show any notable improvement in the leakage current density. The relatively large leakage current density in the NaBEuTi thin film can be well correlated with the poor surface morphology of the thin film, as evident from Fig. 2.

The origin of the leakage current observed in these thin films was investigated by studying leakage current mechanisms using logarithmic plots of leakage current densities (J) versus applied electric field (E) (inset of Fig. 3). Ohmic conduction (S∼1) was found to be the main conduction mechanism at low electric field, which can be theoretically expressed by followings [21];

$$J_{Ohm} = e\mu N_e E \ , \tag{1}$$

where e is the electron charge, μ is the free carrier mobility, N_e is the density of the thermally stimulated electrons and E is the applied electric field. An observation of Ohmic conduction for all the thin films in the low electric field region implied that the leakage current in this region was due to the flow of thermally injected electrons [21]. The transitions from Ohmic conduction to space charge limited (SCL) conduction and to trap-filled limited (TFL) conduction were observed when the applied electric field was increased.

Conduction mechanism changes were found at 18, 22 and 25 kV/cm for the NaBEuTi, NaBGdTi and NaBDyTi thin films, respectively, from Ohmic to SCL conduction by changing S∼1 to S∼2. The SCL conduction occurs when the density of free electrons due to free carrier injection becomes larger than the density of thermally stimulated electrons. The SCL conduction can be expressed as followins [21];

$$J_{SCL} = \frac{9\mu\varepsilon_0\varepsilon_r\theta}{8}\frac{V^2}{d^3} \ , \tag{2}$$

where V is the applied voltage, ε_o is the permittivity of free space, ε_r is the static dielectric constant, d is the thickness of thin film and θ is the ratio of the total density of free electrons to the trapped electrons. Another slope changes from ∼2 to ∼3 were found at 33, 33 and 37 kV/cm of applied electric field for the NaBEuTi, NaBGdTi and NaBDyTi thin films, respectively. This result implied SCL conduction along with some other unknown conduction mechanisms [21].

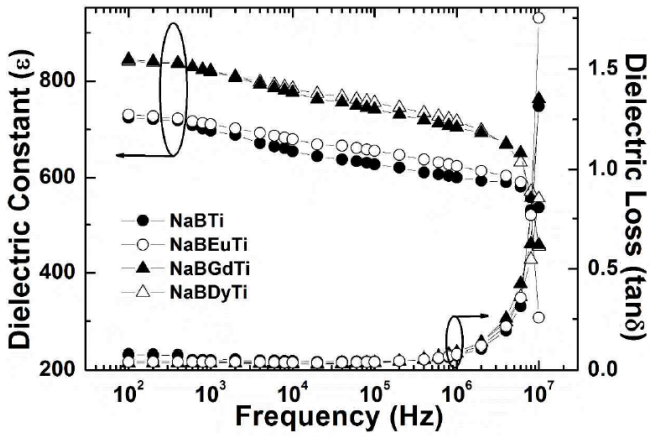

Fig. 4. Frequency-dependent dielectric properties of NaBTi, NaBEuTi, NaBGdTi and NaBDyTi thin films.

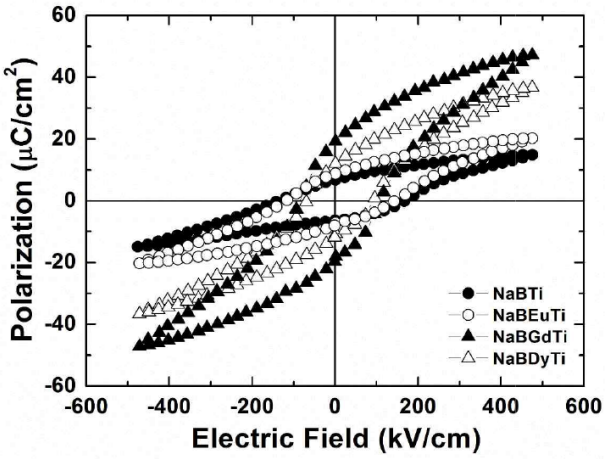

Fig. 5. Polarization-electric field ($P-E$) hysteresis loops of NaBTi, NaBEuTi, NaBGdTi and NaBDyTi thin films.

For the NaBTi thin film, TFL conduction mechanism with an abrupt increase in the leakage current was observed in the higher electric field region, in which the slope was found to be greater than 9. The onset of the TFL conduction in the NaBTi thin film was observed at an applied electric field of 125 kV/cm. The leakage current for TFL conduction can be theoretically expressed by [22,23]

$$J_{TFL} = K\left(\frac{V^{l+1}}{d^{2l+1}}\right) \ , \tag{3}$$

where $K = e^{1-l}\mu N_\nu \left(\frac{2l+1}{l+1}\right)^{l+1}\left(\frac{l}{l+1}\frac{\varepsilon_0\varepsilon_r}{N_t}\right)^l$, $l = (T_t/T)$, T_t is the temperature parameter characterizing the trap distribution, T is the absolute temperature, N_ν is the density of the states in the valence band and N_t is the trap density. The leakage current caused by the TFL conduction was attributed to the flow of excess free charge carriers that remained after filling all the available traps in the NaBTi thin film.

Fig. 4 exhibits dielectric properties of the films measured in the frequency ranges of $10^2 \sim 10^7$ Hz. The measured dielectric constants and dielectric losses of the NaBTi, NaBEuTi, NaBGdTi and NaBDyTi thin films were 697 and 0.050, 710 and 0.041, 819 and 0.034 and 829 and 0.035, respectively, which were measured at 1 kHz. The low dielectric loss values of the NaBGdTi and the NaBDyTi thin films may indicate a low vacancy concentration caused by oxygen and bismuth in these thin films. These vacancies, which are called as space charge components, can be directly related to the dielectric loss. For ferroelectric thin films, a large electrical loss generally occurs due to excessive oxygen vacancies [24].

The ferroelectric properties of the thin films were characterized by studying $P-E$ hysteresis loops, which are measured at room temperature (Fig. 5). The results of this study clearly revealed that the Eu^{3+}, Gd^{3+} and Dy^{3+}-ions used for the doping purpose significantly enhanced the ferroelectric properties, which can be primarily referred to as large ferroelectric remnant polarization and low coercive electric field of the $Na_{0.5}Bi_{4.0}RE_{0.5}Ti_4O_{15}$ thin films. The remnant polarization and the coercive electric field values of the NaBTi, NaBEuTi, NaBGdTi and NaBDyTi thin films, measured at a maximum applied electric field 475 kV/cm, were 13.1 μC/cm^2 and 308 kV/cm, 15.9 μC/cm^2 and 257 kV/cm, 37.4 μC/cm^2 and 187 kV/cm and 23 μC/cm^2 and 164 kV/cm, respectively. For the $Na_{0.5}Bi_{4.0}RE_{0.5}Ti_4O_{15}$ thin films, the enhanced ferroelectric properties can be related to a decrease in the number of oxygen vacancies and the structural distortion caused by the incorporation of RE-ions into the Bi-site [17,18]. The structural distortion was evident from the slight changes in the XRD patterns of the $Na_{0.5}Bi_{4.0}RE_{0.5}Ti_4O_{15}$ thin films. Moreover, it has been well documented that the phenomena of domain pinning assimilated by the existence of large concentration of oxygen vacancies can act as an obstacle for the domain switching in the ferroelectric thin films and low remnant polarization [17,25]. The results observed in the thin films were also well correlated with the leakage current density. The NaBTi and the NaBEuTi thin

films showed large leakage current densities, low remnant polarizations and large coercive fields. On the other hand, the Gd-doped NaBGdTi thin film showed large remnant polarization, which can be correlated with the lowest leakage current density.

IV. CONCLUSION

The ferroelectric $Na_{0.5}Bi_{4.5}Ti_4O_{15}$ and the $Na_{0.5}Bi_{4.0}RE_{0.5}Ti_4O_{15}$ (RE = Eu, Gd and Dy) thin films were prepared on Pt(111)/Ti/SiO_2/Si(100) substrates by using a CSD method. Based on the measured ferroelectric and electrical properties, Eu, Gd and Dy are useful to improve ferroelectric properties of the layered $Na_{0.5}Bi_{4.5}Ti_4O_{15}$ thin films. The improvements in the electrical and the ferroelectric properties of the Eu, Gd and Dy-doped $Na_{0.5}Bi_{4.0}RE_{0.5}Ti_4O_{15}$ thin films were due to the decrease in the number of oxygen vacancies and the structural distortion caused by the doping of these RE-ions into Bi-site. Especially, the Gd-doped $Na_{0.5}Bi_{4.0}Gd_{0.5}Ti_4O_{15}$ thin film exhibited a large value of ferroelectric polarization ($2P_r$) of 37.4 $\mu C/cm^2$ at a maximum applied electric field of 475 kv/cm. Furthermore, the lowest value of the leakage current density of 6.12×10^{-7} A/cm^2 at an applied electric field of 100 kV/cm and a low dielectric loss of 0.034 at 1 kHz were measured for the Gd-doped $Na_{0.5}Bi_{4.0}Gd_{0.5}Ti_4O_{15}$ thin film.

ACKNOWLEDGEMENTS

This research was supported by Basic Science Research Program through the National Research Foundation of Korea (NRF) funded by the Ministry of Education, Science and Technology (2011-0030058). W. J. Kim appreciates the partial financial support from Changwon National University (2017).

REFERENCES

[1] C. A. P. Araujo, J. D. Cuchiaro, L. D. McMillan, M. C. Scott and J. F. Scott, Nature **374**, 627 (1995).

[2] U. Chon, H. M. Jang, M. G. Kim and C. H. Chang, Phys. Rev. Lett. **89**, 087601 (2002).

[3] A. Z. Simões, C. S. Riccardi, A. H. M. Gonzalez, A. Ries and E. Longo *et al.*, Mater. Res. Bull. **42**, 967 (2007).

[4] M. L. Calzada, R. Jiménez, A González and J. Mendiola, Chem. Mater. **13**, 3 (2001).

[5] X. P. Jiang, X.-L. Fu, C. Chen, N. Tu and M.-Z. Xu *et al.*, J. Adv. Ceram. **4**, 54 (2015).

[6] C.-M. Wang, J.-F. Wang, S. Zhang and T. R. Shrout, J. Appl. Phys. **105**, 094110 (2009).

[7] D. Gao, K. W. Kwok and D. Lin, Curr. Appl. Phys. **11**, S124 (2011).

[8] C.-M. Wang, J.-F. Wang, Z.-G. Gai, M.-L. Zhao and L. Zhao, *et al.*, Mater. Chem. Phys. **110**, 402 (2008).

[9] C.-M. Wang and J.-F. Wang, Appl. Phys. Lett. **89**, 202905 (2006).

[10] S. Ikegami and I. Ueda, Jpn. J. Appl. Phys. **13**, 1572 (1974).

[11] V. S. Kopp, V. M. Kaganer, J. Schwarzkopf, F. Waidick and T. Remmele *et al.*, Acta Cryst. A **68**, 148 (2012).

[12] E. C. Subbarao, J. Phys. Chem. Solids **23**, 665 (1962).

[13] F. Qiang, J.-H. He, J. Zhu and X.-B. Chen, J. Solid State. Chem. **179**, 1768 (2006).

[14] U. Chon, J. S. Shim and H. M. Jang, J. Appl. Phys. **93**, 4769 (2003).

[15] T. Kojima, T. Sakai, T. Watanabe, H. Funakubo and K. Saito *et al.*, Appl. Phys. Lett. **80**, 2746 (2002).

[16] H. Sun, X. B. Chen, J. Zhu, J. H. He and Y. F. Qian *et al.*, J. Sol-Gel. Sci. Technol. **43**, 125 (2007).

[17] B. H. Park, B. S. Kang, S. D. Bu, T. W. Noh and J. Lee *et al.*, Nature **401**, 682 (1999).

[18] A. Garg, X. Hu and Z. H. Barber, Ferroelectr. **328**, 93 (2005).

[19] X. G. Tang, J. Wang, X. X. Wang and H. L. W. Chan, Chem. Mater. **16**, 5293 (2004).

[20] D. H. Kang and Y. H. Kang, J. Microelectron. Packag. Soc. **20**, 25 (2013).

[21] C. Wang, M. Takahashi, H. Fujino, X. Zhao and E. Kume *et al.*, J. Appl. Phys. **99**, 054104 (2006).

[22] A. Roy, S. Maity, A. Dhar, D. Battacharya and S. K. Ray, J. Appl. Phys. **105**, 044103 (2009).
[23] D. S. Shang, Q. Wang, L. D. Chen, R. Dong and X. M. Li *et al.*, Phys. Rev. B **73**, 245427 (2006).
[24] I. Coondoo, A. K. Jha and S. K. Agarwal, J. Eur. Ceram. Soc. **27**, 253 (2007).
[25] J. F. Scott and M. Dawber, Appl. Phys. Lett. **76**, 3801 (2000).